Journal of Applied Polymer Science

Positive-Tone, Aqueous-Developable, Polynorbornene Dielectric: Lithographic, and Dissolution Properties

Brennen K. Mueller,[1] Edmund Elce,[2] Angelica M. Grillo,[1] Paul A. Kohl[1]
[1]School of Chemical and Biomolecular Engineering, Georgia Institute of Technology, Atlanta, Georgia 30332-0100
[2]Promerus LLC, Brecksville, Ohio 44141
Correspondence to: P. A. Kohl (E-mail: paul.kohl@chbe.gatech.edu)

ABSTRACT: A positive-tone, aqueous base soluble, polynorbornene (PNB) dielectric formulation has been developed. The photolithographic solubility switching mechanism is based on diazonaphthoquinone (DNQ) inhibition of PNB resin functionalized with pendent fluoroalcohol and carboxylic acid substituents. The optical contrast (at 365 nm) was found to be 2.3. The maximum height-to-width aspect ratio of developed line and space features was 3 : 2. The sensitivity, D_{100}, of a formulation containing 20 pphr of DNQ photoactive compound (PAC) was calculated to be 408 mJ cm^{-2}. The effects of the PAC molecule structure on miscibility and dissolution of the photosensitive films in aqueous base developer were studied. The effect of the monomer composition of the PNB polymer on the dissolution rate of the formulated PNB resin was evaluated. A unique dissolution and swelling behavior was observed. The effect is attributed to a copolymer synthesized with two monomers each of which is susceptible to deprotonation in aqueous base. FTIR measurements showed that the pure PNBFA has a small percentage of free hydroxyl groups, which did not change appreciably by the addition of PAC to the mixture. © 2012 Wiley Periodicals, Inc. J. Appl. Polym. Sci. 000: 000–000, 2012

KEYWORDS: dielectric; DNQ; photosensitive

Received 31 January 2012; accepted 10 May 2012; published online
DOI: 10.1002/app.38055

INTRODUCTION

Polymers are widely used in microelectronic device fabrication as temporary masking materials and permanent insulators.[1–4] Polymeric dielectrics can provide a low-cost alternative to inorganic materials, which often require complex deposition steps and exposure to aggressive wet or dry etch conditions. Polymeric materials can also have lower elastic modulus and higher toughness than inorganic materials. One area of interest is the use of polymers as low-permittivity, permanent dielectrics for on-chip, and substrate packaging applications. The use of low-permittivity materials in integrated circuits can serve to decrease electrical losses between interconnects, allowing for more tightly packed and energy-efficient electronic devices.

There is a need for thick-film, positive-tone, photosensitive dielectrics for packaging, and wafer passivation applications.[1,5,6] Positive-tone materials are better suited for interlevel dielectrics and passivation layers over substrates because lithographic masks have reduced sensitivity to particulates (dark field masks) and there is less swelling than with negative-tone systems. Positive-tone materials require fewer photochemical reactions to form vias through passivation layers. It is especially attractive to be able to develop the latent image in an aqueous solution (e.g., aqueous base), compared with solvent-developed systems, because the process is more environmentally friendly than solvent-based developers.

Polynorbornene (PNB) based polymers have been investigated as a dielectric material.[4,7,8] PNB itself has a saturated hydrocarbon backbone, which engenders a low dielectric constant, low moisture uptake, high glass transition temperature, and good mechanical properties.[7] PNB can also be functionalized with hydroxyl, carboxylic acid, and epoxy functionalities, which allows for solubility in aqueous base, a high degree of crosslinking, and excellent adhesion to a variety of substrates.[4,7] Functionalized PNB polymers have been synthesized by addition copolymerization of cyclic olefins by group VIII transition metal catalysts; this polymerization method produces a saturated, high molecular weight polymer that is soluble in a range of organic solvents.[9]

The polymers used in this study were homopolymers or copolymers of functionalized PNB monomers.[10] Functionalized monomers, a norbornene fluoroalcohol (NBFA) and a norbornene carboxylic acid (NBCBA), impart solubility in aqueous base. The NBCBA functionality also provides sites for polymer crosslinking with small-molecule, multifunctional epoxy additives.

Applied Polymer SCIENCE

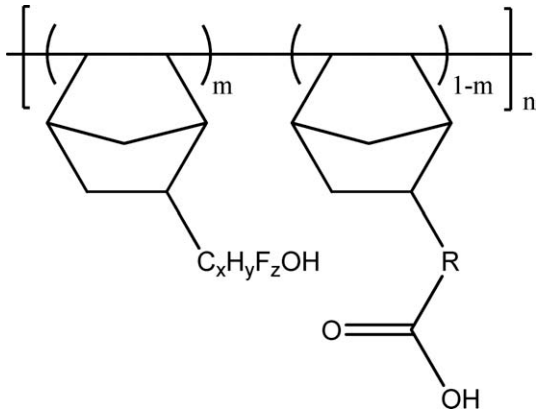

Figure 1. Functionalized PNB copolymer.

The chemical structure of P(NBFA-NBCBA) is given in Figure 1. Cross-linking of the polymer results in a high molecular weight, thermoset with stable electrical properties. In the positive-tone system, crosslinking can be thermally induced during the thermal cure after development of the latent image. Rajarathinam and Raeis-Zadeh have studied negative-tone forms of PNB for packaging applications and have reported good mechanical and electrical properties.[4,8]

The fluoroalcohol substituent is useful in creating positive-tone photosensitive polymers because its pK_a is similar to that of the phenolic hydroxyl group of a novolac resin.[11] In a novolac resist, diazonaphthoquinone (DNQ) is used as an inhibitor to prevent aqueous base dissolution of the unexposed portions of the novolac resin during the development of the exposed regions.[12–14] Reiser suggests that DNQ causes extensive hydrogen bonding between the phenolic hydroxyl groups on the polymer, lowering the tendency of these groups to deprotonate when exposed to base.[13] Exposure of a resin containing DNQ to ultraviolet (UV) light induces a chemical reaction known as the Wolff rearrangement to form an indene carboxylic acid (ICA). The formation of the ICA disrupts the hydrogen bonding dissolution inhibition mechanism and increases the dissolution rate of the novolac mixture in aqueous base. In this study, DNQ was used to inhibit dissolution of PNB, just as it does with novolac.

A working positive-tone functionalized PNB resin has been demonstrated and its lithographic properties are reported here. The effect of the photoactive compound (PAC) on the miscibility with the PNB matrix and dissolution of the mixture have been studied. It is shown that the ballast portion of the PAC strongly affects miscibility of the PAC with the PNB polymer resin. Furthermore, effects of the monomer ratios in PNB copolymers on the dissolution behavior in aqueous base have been studied by quartz crystal microbalance (QCM) measurements. This data is compared to Fourier transform infrared spectroscopy (FTIR) measurements of hydrogen bonding.

EXPERIMENTAL

The PNB polymers were supplied by Promerus LLC (Brecksville, OH). PNB-A and PNB-B are 75/25%, and 90/10% random copolymers of P(NBFA-NBCBA), respectively. They were dissolved in propylene glycol monomethyl ether acetate (PGMEA) at concentrations of 16–30 wt %. PNB-C was pure PNBFA. Three PACs were used in this study, identified as PAC1, PAC2, and PAC3 (Figure 2). All ballast portions of the PACs contained two or more hydroxyl groups, which were esterified with 2,1,5-DNQ sulfonic acid to have two DNQ moieties per photoactive molecule, on average. The PAC1 ballast molecule had two hydroxyl groups esterified at ~100% (i.e., two DNQ moieties per molecule). PAC2 was a 2,4-dihydroxybenzophenone-type ballast molecule with two hydroxyl groups, also esterified at ~100%. PAC3 was a trisphenol-PA-type ballast molecule, of similar molecular weight to PAC1, with three hydroxyl groups, esterified at ~67%. Formulations containing PGMEA, PNB polymer, and various loadings of PAC were mixed by ball-milling overnight. AZ P4620 (AZ Electronic Materials) is a thick-film, novolac-based photoresist.

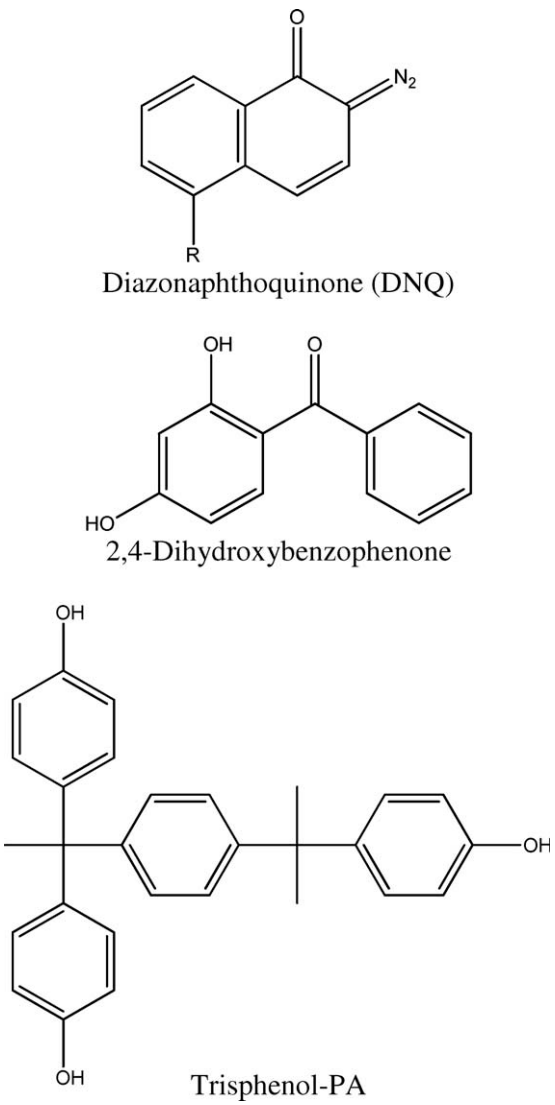

Figure 2. Chemical structure of (a) diazonaphthoquinone, (b) PAC2 ballast molecule, and (c) PAC3 ballast molecule.

Thin films were cast by spin-coating using a CEE 100CB spinner at speeds of 2000–3000 rpm for 60 sec. Films thicker than 5 μm were soft baked on a hot plate for 2 min at 100°C. Thinner films were soft baked for 1 minute at 100°C. Film thicknesses were measured on a Veeco Dektak profilometer. Samples were exposed using an Oriel Instruments flood exposure source with a 1000 W Hg(Xe) lamp filtered to provide 365 nm radiation. The films were developed with MF-319 (Shipley), a 0.26*N* tetramethylammonium hydroxide (TMAH) aqueous base developer. Films were developed in an agitated puddle fashion. Contrast, sensitivity, and aspect ratio experiments were performed by exposing 8–10 μm thick films in soft contact with a variable-density optical mask (Opto-line International Inc). The films were coated on ⟨100⟩ silicon wafers that were treated with (3-aminopropyl) triethoxysilane as a primer to improve adhesion. Contrast (γ) values were obtained by plotting the normalized film thickness after an aqueous base develop against the logarithmic exposure dose and fitting the curve with a linear least squares fit at the points closest to D_{100}. D_{100} is defined as the minimum dose at which 100% of the film is removed for a positive-tone resist. This point is the *x*-intercept of the contrast curve, where the film thickness is equal to zero. D_{100} is taken as a measure of sensitivity. D_0 is defined as the minimum dose at which 100% of the film remains after development. Since positive resists have a finite solubility even in the unexposed, the value of D_0 was calculated by extrapolating the slope of the contrast curve to a normalized thickness of 1.

$$\gamma = \frac{1}{\log(D_{100}/D_0)} \tag{1}$$

The aspect ratio is the ratio of the feature height-to-width for the smallest features that retained 100% of the unexposed film thickness. These widths and thicknesses were measured by scanning electron microscopy (SEM), using a Zeiss Ultra 60 SEM. The SEM samples were sputtered with 18–20 nm of gold using a Hummer 5 Gold Sputter tool to prevent charging of the film during examination.

Ultraviolet-visible spectroscopy (UV–vis) absorbance measurements were taken with a Hewlett Packard 8543 UV–vis spectrophotometer. Films for UV–vis measurements were spin coated on glass microscope slides. The background spectrum of the slide was subtracted from the sample spectrum. Absorbance values at 365 nm were recorded, and film thicknesses were measured to calculate the absorption coefficient, α. FTIR measurements were obtained using a Magna 560 FTIR (Nicolet Instruments). FTIR samples were coated on a KBr disk. The absorbance data was averaged over 500 scans at a resolution of 2 cm^{-1}. FTIR spectra were automatically baseline corrected, and the peak areas were calculated by a least squares method, fitting Gaussian peaks.

Dissolution rate experiments were obtained using a QCM200 QCM system (Stanford Research Systems). Samples were spin-coated onto a 1″ QCM with 5 MHz unloaded resonant frequency and 0.4 cm^2 active surface area. Coated QCMs were developed with MF-319 in a 125 μL flow cell connected to a ~800 μL min^{-1} peristaltic pump (Thermo Scientific). The flow path was equipped with a manual valve positioned ~2 in. from the inlet of the flow cell to control selection between water and MF-319. The polymer-coated QCM samples were first equilibrated in water before introduction of the aqueous base developer to minimize sharp frequency and resistance changes that result from immersion into a viscous medium from air. Mass changes (Δm) were obtained by correlation of the resonant frequency change (Δf) using the Sauerbrey equation, eq. (2).

$$\Delta f = -\frac{2f_0^2}{A\sqrt{\rho_q \mu_q}}\Delta m \tag{2}$$

where f_o is the resonant frequency of the unloaded quartz crystal, A is the active area between the gold electrodes, ρ_q is the density of quartz, and μ_q is the shear modulus of quartz. The thickness was calculated by taking the density of the polymer to be 1.3 +/−0.05, as obtained from measuring thickness and mass.

Table I. PNB Formulations

Name	Polymer	PAC Type	DNQ Loading
Formulation X	PNB-A	PAC1	20 pphr
Formulation Y	PNB-A	PAC1	25 pphr

RESULTS AND DISCUSSION

Lithographic Properties of Positive-Tone PNB Formulations

The contrast, sensitivity, and maximum obtainable aspect ratio were evaluated for two different PNB/PAC formulations, Formulations X and Y, as given in Table I. The PAC concentration is given in parts PAC per hundred parts PNB mass (pphr). For example, a 20 pphr PAC1 mixture is 20 g of PAC1 for each 100 g of PNB polymer. The contrast and sensitivity of these two formulations were evaluated after development in 0.26 and 0.195*N* TMAH. Samples were developed for 5 sec longer than the time required to remove all film in the region of highest exposure dose. It was always the case that the regions of the film exposed to a dose $>D_{100}$ dissolved at the same rate. Contrast curves of both formulations developed in 0.26*N* TMAH is shown in Figure 3. The sensitivity of these two formulations, as given by the D_{100} value for Formulations X and Y, were 408 and 617 mJ cm^{-2}, respectively. The sensitivity is a function of the PAC loading, but it is not directly proportional to the PAC loading because of inefficient absorption of light (the quantum efficiency of DNQ is less than unity[15]) and photobleaching in thick films. Photobleaching is a decrease in absorption coefficient because of the chemical reaction of a DNQ after exposure to UV radiation. The D_o values are almost identical for the two formulations. The contrast values of Formulations X and Y were calculated to be 2.3 and 1.5, respectively, in 0.26*N* TMAH. The decrease in contrast with increased PAC1 loading is a result of a higher D_{100} value for Formulation Y. A small discontinuity in the contrast curves can be seen in Figure 3 around 200 mJ cm^{-2} for both formulations. The cause of this is unclear now but will be further investigated.

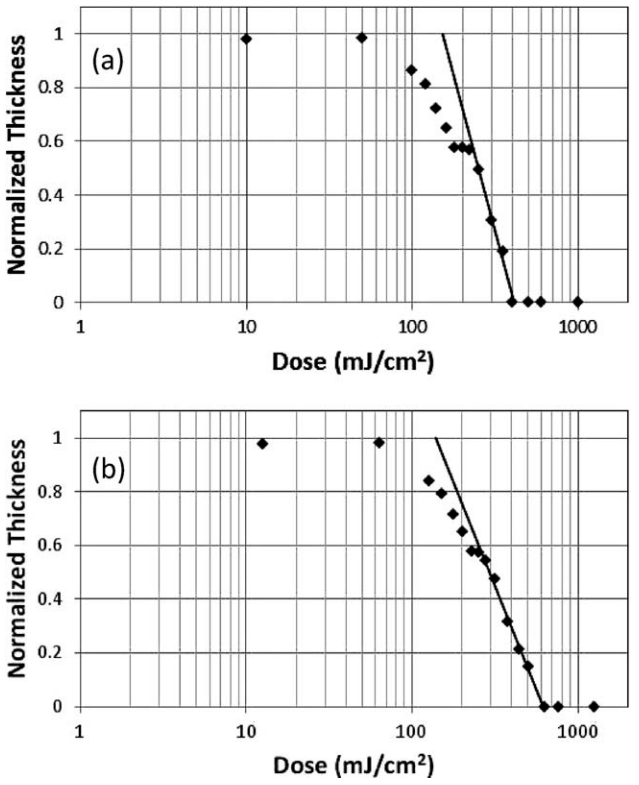

Figure 3. Contrast curves for (a) Formulation X and (b) Formulation Y. Both were developed in 0.26*N* TMAH.

The contrast values for Formulations X and Y in 0.195 and 0.26*N* TMAH are tabulated in Table II. At the lower developer concentration, 0.195*N* TMAH, the contrast value for Formulation X dropped slightly to 2.0 whereas the contrast of Formulation Y remained unchanged at 1.5. The D_{100} value of each formulation was independent of the base concentration in the developer. This result shows that at the D_{100} dose, a critical fraction of the DNQ moieties in the deepest regions within the film, that is, near the polymer–substrate interface, have been converted to ICA. This critical fraction is the amount of conversion required for the film to be soluble in aqueous base. These results indicate that this critical level of conversion of DNQ to ICA is not dependent on the base concentration over the range of concentrations used here.

Figure 4 shows SEM images of Formulation Y developed in 0.26*N* TMAH. The film thickness in Figure 4 is 9.2 μm. A dark field exposure showing line and space features in the film are shown in Figure 4(a). This formulation exhibits slight rounding at the corners of the structures and somewhat sloped sidewall profiles. The smallest features that show no loss of the fidelity of the lines are the 12 μm pitch trenches. Almost no material remains for the 6 μm pitch features. Figure 4(b) shows the light field image where freestanding structures were formed on the substrate. The rounded edges and sloped sidewalls of the structures are more apparent in the light field exposure. The 12 μm pitch structures were the smallest features resolved in the light-field sample. The maximum aspect ratio (height-to-width) achieved was 3 : 2. The next smallest feature size, which was not fully resolved, was the 10 μm pitch structures. These features had rounded tops, indicating erosion of the unexposed resin at the top of the line features.

Effect of PAC Molecular Structure on Miscibility and Dissolution

Two other PACs were investigated with the PNB polymer. The first, PAC2, a difunctional hydroxybenzophenone-type DNQ, is often used in novolac photoresists. All formulations containing PAC2 had poor miscibility resulting in visible precipitates, which were observed using an optical microscope after spin coating, as shown in Figure 5. The particle sizes ranged from 1 µm to more than 100 µm in diameter. A flaky brown film around the features was formed when the films were developed in 0.26*N* TMAH. This brown film also formed in the light field region when large area films were exposed to UV radiation. The brown film appeared within the first few seconds of development when the exposure dose was low, 50–250 mJ cm^{-2}, for 15 μm thick films. It was also observed in a sample receiving a gradient exposure dose that the brown film appeared during development when structures of varying exposure dose were developed across the same sample. The brown film took longer to appear at high exposure doses (>250 mJ cm^{-2} in 15 μm films). Finally, at a sufficiently high dose, the brown film did not appear in the light field region of the exposed films. However, the brown film still formed at feature edges when the exposure dose was high. This is because the optical dose at the transition region from the irradiated to unirradiated region at the edge of the features was less than the full exposure dose and within the values cited above for producing a brown film.

Formulations were made of PNB-C (i.e., PNBFA) and PAC2. Films produced from these mixtures showed the same random precipitate. A similar brown color was observed during development, but it formed more slowly with time, compared with films made from PNB-A. It was also observed that the dissolution rate of PNB-C in base was much slower than that of PNB-A.

Table II. Contrast and Sensitivity Values

Formulation	Base Normality	Develop Time (s)	Contrast	D_0 (mJ cm^{-2})	D_{100} (mJ cm^{-2})
X	0.26	76	2.3	153	408
X	0.195	105	2	131	408
Y	0.26	79	1.5	138	618
Y	0.195	141	1.5	139	616

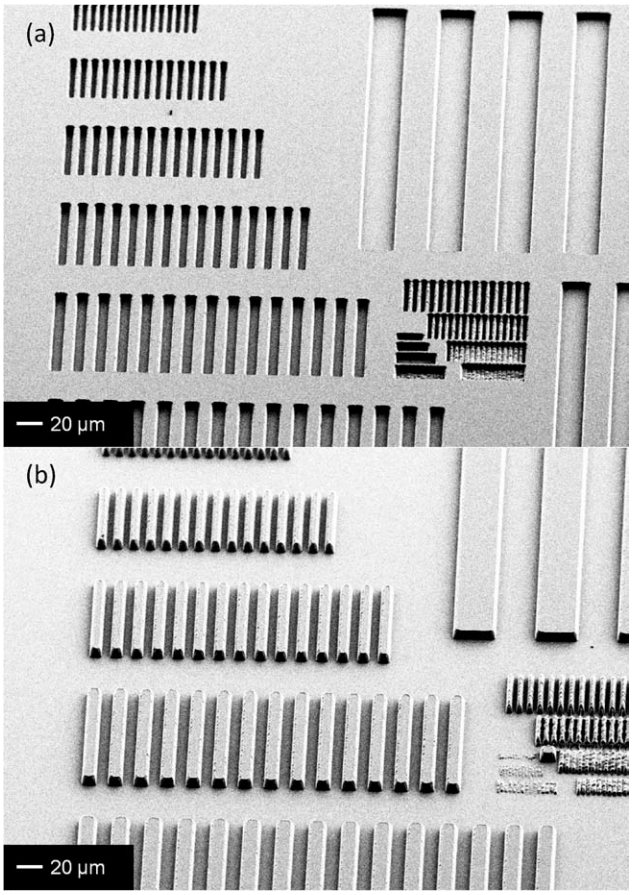

Figure 4. SEM images of Formulation X. (a) trenches in the polymer film and (b) hills on the substrate.

Mixtures of PAC3 and PNB-A in PGMEA appeared to be completely miscible. However, the solvent cast films became opaque almost immediately during soft baking at 100°C. Upon closer investigation with an optical microscope, it was seen that this opacity was a result of phase segregation. This effect was worse in formulations with higher PAC3 loading. These observations indicate that PAC3 has limited miscibility with PNB-A. Development of these films in 0.26*N* TMAH produced the same brown color in the spin-cast film as previously noted. However, the brown film formed in PNB-A with PAC3 was less flaky and more gel-like than the other brown films, causing it to smear over the sample. The brown film residue produced from PNB-A with both PAC2 and PAC3 are shown in Figure 6.

PNB-C/PAC3 formulations were also made. Films of these mixtures showed phase segregation to a greater extent than films with PNB-A. The brown color appeared more slowly in these formulations compared with the films made with PNB-A. The dissolution rate of the films made from PNB-C/PAC3 was very slow. The higher degree of phase segregation with PNB-C, compared with films made with PNB-A implies that the NBCBA (25% in PNB-A) is more miscible with PAC3 than NBFA. That is, the carboxylic acid functionality of the polymer improves the polymer/PAC miscibility and raises the dissolution rate. The increased miscibility between the PAC and PNB is likely caused by the increased polarity of the NBCBA compared with the NBFA. The polar DNQ moiety is then more miscible with polymers that contain a higher content of polar NBCBA.

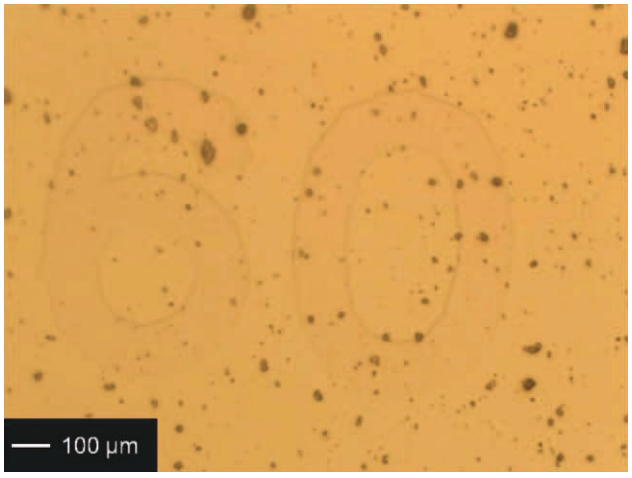

Figure 5. Defects in a film of PNB-A and PAC2. [Color figure can be viewed in the online issue, which is available at wileyonlinelibrary.com.]

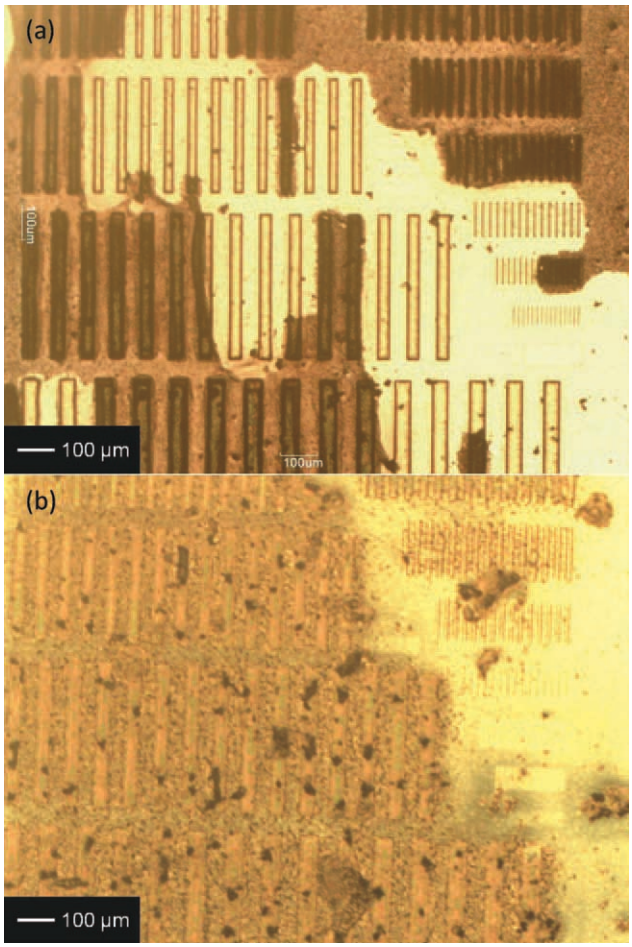

Figure 6. Brown residue from (a) PNB-A and PAC2 and (b) PNB-A and PAC3. [Color figure can be viewed in the online issue, which is available at wileyonlinelibrary.com.]

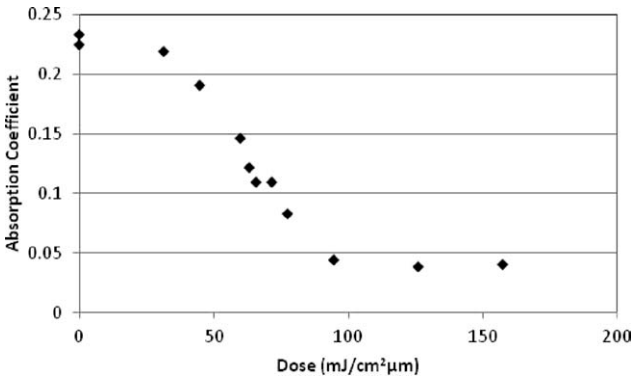

Figure 7. Absorption coefficient at 365 nm of a 27 pphr PAC2 in Polymer A plotted versus exposure dose.

UV–vis spectroscopy was used to understand the extent of photobleaching. PNB-A films with 27 pphr PAC2 were coated to a thickness of 16–17 μm. Figure 7 shows the absorption coefficient for the PNB-A/PAC2 formulation plotted against the exposure dose per micrometer of film thickness. The relationship between dose and film thickness is nearly linear over a small range of thicknesses. The results show that the absorption coefficient for the unexposed film is 0.23, with a gradual decrease in the absorption coefficient of the film with exposure dose. This decrease in absorption coefficient continues until the dose reaches ~95 mJ cm^{-2} μm^{-1} at which point the absorption coefficient becomes 0.04. Above ~95 mJ cm^{-2} μm^{-1}, there is little change in the absorption coefficient with UV dose. Initially, the optical dose deep in the film is low due to the high absorbance in the upper regions of the film. As the upper layer of the film is exposed, its absorbance decreases which gives a higher UV intensity deep in the film. Hence, it is possible that a film consists of two states during and after exposure if it is of sufficient thickness and low dose: (i) fully exposed and (ii) underexposed. The fully exposed region has been exposed to enough UV radiation to convert all DNQ to ICA, whereas the underexposed region has not been fully exposed and thus contains both DNQ and ICA. A dose of 95 mJ cm^{-2} μm^{-1} is assumed to be value at which the entire film is fully exposed. This value is dependent on the PAC loading in the film.

The dose needed for full exposure correlated well to the dose at which the brown film no longer formed during development in 0.26*N* TMAH. From this result, it was concluded that the brown film was seen during the develop step only when both DNQ and ICA were present in the film. Others have shown that reactions of DNQ and ICA are possible, several of which may have little or no solubility in aqueous base.[16,17] It is speculated that the brown film is the product of a reaction of DNQ and ICA, resulting in an insoluble, high molecular weight compound. This product would explain why no brown film is seen in fully exposed samples. Further, this explains why the brown film is more gel-like for formulations with PAC3. This is because the PAC3 ballast molecule initially has three hydroxyl groups but is only esterified with two 2,1,5-DNQ sulfonic acid groups. The nonesterified hydroxyl site on the ballast portion of the PAC3 molecule can react with base and make the brown film swell in aqueous base. From these results, the factors that most affect the lithographic properties of the PAC/PNB mixtures are PNB-PAC miscibility and degree of PAC substitution. The degree of immiscibility between PNB and the PAC causes film defects to occur that decrease product yield. It was also determined that PACs with 100% esterification perform better than the PAC with 67% esterification due to the reactivity of unesterified hydroxyl groups with base.

The hypothesis that a DNQ/ICA reaction product occurs implies that the brown film can be formed in any DNQ-containing photoresist, as long as the dose is sufficiently low and the dissolution rate is sufficiently high. In an effort to investigate this effect, AZ P4620 was spin-coated to 14 μm thickness and processed by the same methods as the PNB formulations. At exposure doses of <25 mJ cm^{-2}, the same brown color film was seen during the initial stages of development in 0.26*N* TMAH. At this low dose, it is likely that the region of the film closest to the substrate contained both DNQ and ICA. The surface region is also exposed to the highest concentration of base during development.

Effect of Copolymer Composition on Dissolution

The PNB copolymers studied in this work are composed of two monomers, each of which is susceptible to deprotonation by aqueous base. Carboxylic acids generally have a pK_a value of 3–4, whereas the fluoroalcohol has a pK_a of 9–10. Thus, it is expected that the deprotonation of NBCBA occurs first (before NBFA) as base penetrates the film and the pH rises. However, since the mol % of NBCBA in PNB-A is only 25%, it is not expected that deprotonation of the NBCBA will result in dissolution of the polymer film. For these reasons, we conclude that PNB copolymers exhibit complex dissolution characteristics.

The dissolution of PNB-A, PNB-B, and PNB-C mixtures were characterized using a QCM to monitor the sample mass as a function of time in the developer. At resonance, the frequency shift of the QCM is proportional to the change in mass, eq. (1). Figure 8(a) shows a typical QCM response, with the observed change in mass plotted versus time. Measuring the slope of this curve during dissolution provides a mass dissolution rate. The thickness dissolution rate can be calculated using the estimated density of the polymer. Figure 8(b) shows the QCM resistance as a function of time for the same sample as in Figure 8(a). This resistance is a measurement of the energy dissipated by the viscous layer on the solid polymer film on the quartz crystal.[18,19] As the polymer takes up aqueous base, a gel layer is formed. The mechanical properties of this gel layer are different from that of the dry film. The magnitude and importance of the gel layer can be qualitatively understood by monitoring the resistance.

The dissolution rate of polymer films was measured and the logarithmic rate was plotted versus PAC concentration in a Meyerhofer-type fashion. These plots are shown in Figure 9 for the three polymer mixtures. The dissolution rates for PNB-A, PNB-B, and PNB-C without additives were found to be 12.2, 8.7, and 5.9 μm min^{-1}, respectively, indicating that a higher percentage of NBCBA in the copolymer increases the dissolution rate in aqueous base. This result was expected because of the higher acidity proton on NBCBA than NBFA. PNB-B and

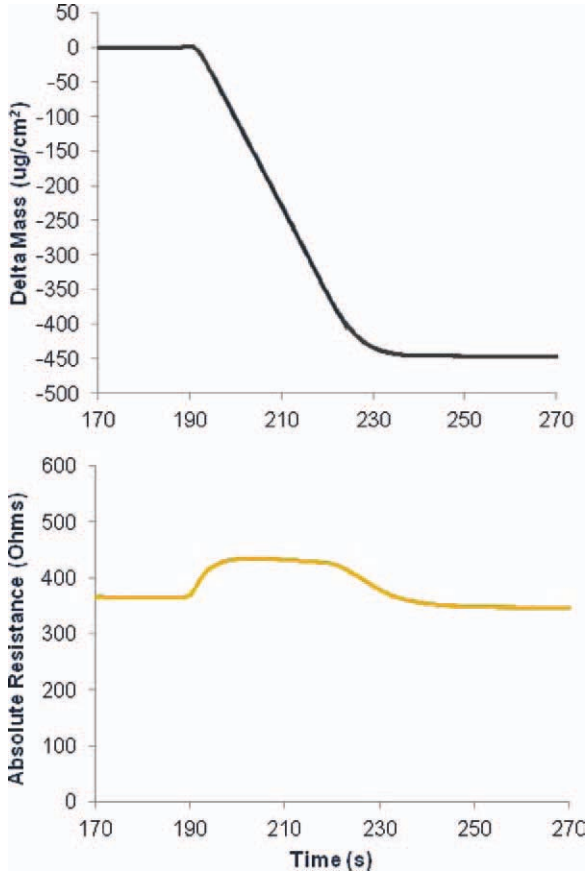

Figure 8. Example QCM traces of (a) mass and (b) resistance of a PNB film. [Color figure can be viewed in the online issue, which is available at wileyonlinelibrary.com.]

PNB-C exhibited a decrease in dissolution rate with increasing PAC1 loading, which is also expected and typical of DNQ-type photoresists. However, these two polymers also showed a decrease in dissolution rate with increasing amounts of ICA (because of exposure to UV radiation), which is not typical for positive-tone, DNQ-based resists.[20] Generally, the dissolution rate of the exposed film remains constant or increases with ICA loading. In this regard, the dissolution of PNB films appears to differ from the dissolution of novolac resists. This may be attributed to a large hydroxyl string reconnection efficiency after exposure originating at the PAC sulfonyl moieties. PNB-A appears to show little change in dissolution rate with increasing PAC1 concentration between the exposed and unexposed films. However, the high resistance value indicates that a substantial gel region has formed during developing. The gel layer is soft enough so that it cannot follow the QCM oscillations without significant energy loss. Thus, the film decouples from the oscillator. We propose that the aqueous base penetration rate into the PNB-A film is faster than the dissolution rate of the film. This results in a net influx of aqueous base into the film causing the film to gel. The increase in resonant frequency of the QCM occurs quickly once the sample is immersed into base. The frequency quickly reaches a steady value; however, the resistance is slower to reach an equilibrium value. This higher resistance indicates that the physical presence of the film causes viscous energy loss even though the QCM frequency shows complete loss of mass.

The dissolution rate of the exposed and unexposed polymer films containing 20 pphr PAC1 were also measured by QCM. PNB-B and PNB-C were found to show similar characteristics. The unexposed films of each formulation showed no measureable change in mass indicating that these films are completely inhibited by the 20 pphr PAC1. After exposure to UV radiation, the films had a finite solubility that is almost two orders of magnitude less than the pure polymer films. Films of PNB-A with 20 pphr PAC1 showed a much different behavior. The observed dissolution rate of the UV-exposed films of PNB-A and 20 pphr PAC1 were calculated to be 8.4 μm min^{-1}. The dissolution rate of this formulation was confirmed by measuring the dissolution rate of films during puddle development.

Unexposed films of PNB-A with 20 pphr PAC1 displayed a different behavior from the similar mixtures with PNB-B or PNB-

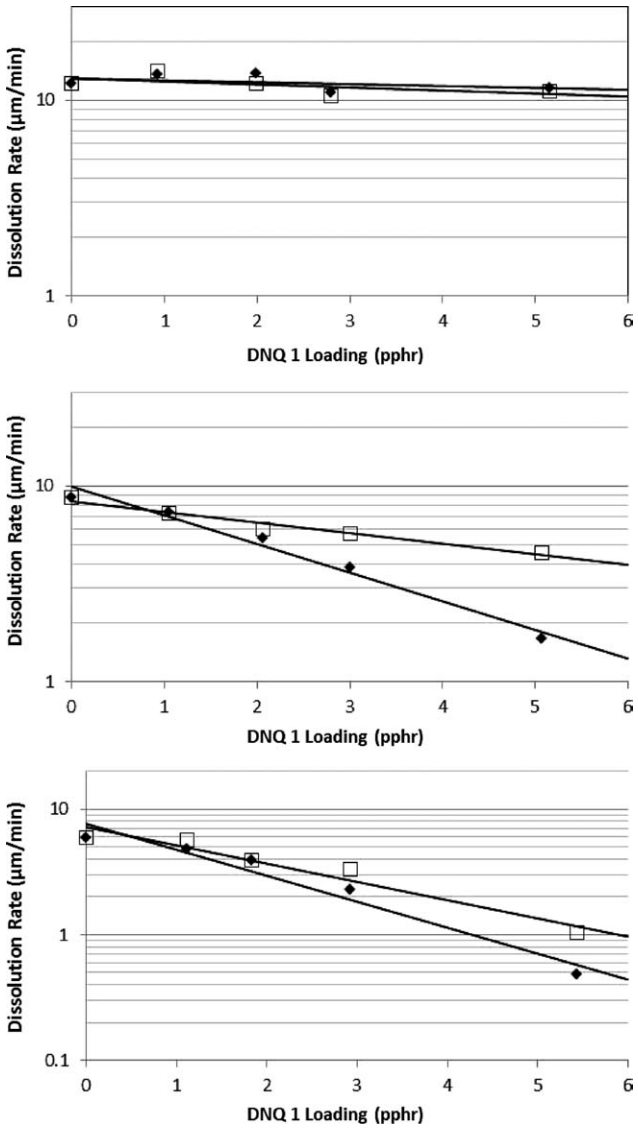

Figure 9. Meyerhofer plots of (a) PNB-A, (b) PNB-B, and (c) PNB-C as a function of PAC1 loading. □ = unexposed; ◆ = exposed.

C. When exposed to aqueous base, the mass and resistance measurements rapidly increased. The resistance for films >200 nm increased to very high values and eventually the QCM stopped oscillating. For this reason, thinner films of PNB-A with 20 pphr PAC1 were cast (~185 nm thick or ~24 μg cm^{-2}). The QCM response of the thin films was monitored during development in aqueous base. A rapid decrease in QCM frequency (indicating an increase in mass) and increase in resistance was again observed. These frequency and resistance values peaked shortly after immersion in aqueous base and then fell. The final, steady-state frequency obtained in aqueous base would correspond to removal of most of the film; however, the final value of resistance was much higher than expected if this were the case. This film was then immersed in water after the exposure to base. If the film had dissolved, there would have been little change in frequency or resistance. Note, only a slight change in frequency and resistance was observed by changing the viscosity of the solution from water to aqueous base for a clean QCM. However, in the case of PNB-A, the change to water caused a large decrease in frequency and increase in QCM resistance. After a long period of time where water flowed through the cell, the frequency reached a value that corresponded to triple the initial mass. The resistance returned to a low value, which was only 22 Ω greater than the initial resistance. Examination of the QCM after removal from the liquid cell indeed showed that undissolved polymer film was still present on the QCM surface. Taken together, these results show that the film swelled in aqueous base to the point of gelation with high-energy loss so that the QCM response no longer reflected the correct mass and eq. (1) could not be used. Once the film was immersed in pure water, the film returned to a rigid state with an increase in mass.

Effect of DNQ on Hydrogen Bonding in PNB Films

Studies of hydrogen bonding in NBFA-containing polymers have been reported by others.[21,22] Similar measurements were performed here to study the effect of PAC loading on the hydrogen bonding in the PNB-C film. FTIR measurements of PNB-C films containing 0, 5, and 20 pphr PAC1 were used to examine the bonding environment and quantity of hydroxyl groups present. The hydroxyl stretching region occurs between 3000 and 3700 cm^{-1}. The peak associated with "free hydroxyl" occurs at 3600 cm^{-1}, whereas the hydrogen-bonded hydroxyl stretch has a broader peak between 3500 and 3300 cm^{-1}. The relative area associated with each peak was used to evaluate the fraction of hydroxyl groups associated with each state. Figure 10 is an FTIR spectrum of a PNB-C (i.e., PNBFA) film, which shows three possible hydroxyl peaks. The data from this study is shown in Table III. In the pure PNBFA film, with no additives, only 10% of the hydroxyl groups are free. This percentage is smaller than in previous studies; however, the soft bake temperature used here was substantially lower than in the previous studies. The films in this work were soft baked at 100°C to avoid significant thermal activation of the DNQ. At this temperature, it is possible that residual solvents remained in the film which affected the hydrogen bonding of the HFI groups.

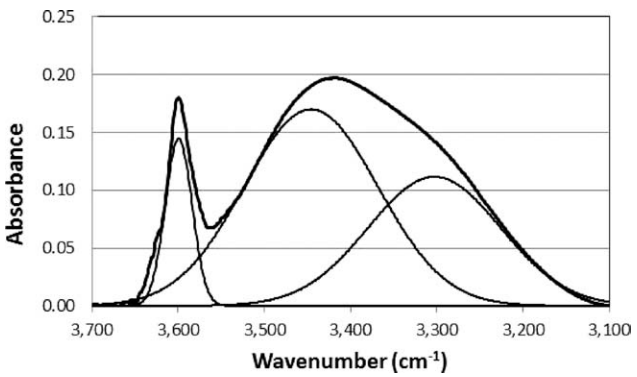

Figure 10. FTIR hydroxyl stretching region of a PNB-C film.

Table III. FTIR Hydroxyl Peak Percentages

PAC1 Loading	3600 cm^{-1}	3450 cm^{-1}	3300 cm^{-1}	Dissolution Rate (μm min^{-1})
0 pphr	9%	55%	36%	5.8
5 pphr (unexposed)	12%	44%	44%	0.48
5 pphr (exposed)	12%	55%	33%	1.0
20 pphr (unexposed)	7%	30%	63%	~0
20 pphr (exposed)	7%	45%	48%	0.18

The addition of 5 pphr PAC1 resulted in a small increase in the free hydroxyl content to 12%. It was expected that a decrease in hydrogen bonding would cause an increase in the dissolution rate. However, the addition of 5 pphr PAC1 to PNB-C lowers the dissolution rate by a factor of 10 compared with films of pure PNB-C. An explanation for this may be that PNB-C has a large degree of hydrogen bonding without additives, and the introduction of large molecule, PACs disrupts the hydrogen bonding. The PAC still lowers the dissolution rate of the film due to the insolubility of the high molecular weight, unexposed PAC in aqueous base. After complete UV exposure, the percentage of free hydroxyl groups remains the same at 12%. However, the dissolution rate more than doubles after exposure. Further, increasing the PAC1 loading to 20 pphr causes the percentage of free hydroxyl groups to decrease to 7%. Again, exposure of this film causes no change in the free hydroxyl peak. In this case, the unexposed film is completely inhibited to development by aqueous base. Exposure of the film causes it to become soluble, although the dissolution rate is very small. The first conclusion made from these results is that pure PNB-C has a large degree of hydrogen bonding without the addition of a PAC. In addition, the addition of a PAC does not change the hydrogen bonding to any appreciable extent. This may indicate that PNBFA does not form hydrogen-bonded strings like novolac resins.[23] The result that UV exposure does not change the degree of hydrogen bonding is likely due to a number of factors. PNBFA already has extensive hydrogen bonding without the addition of DNQ, so the light-induced rearrangement of the carbonyl to a carboxylic acid may not have a significant impact on the total hydrogen bonding effect. Furthermore, sulfonyl groups on the PAC remain unchanged after exposure. Reiser et al. have found that the recombination of hydroxyl strings to

these groups can be high.[20] It was then concluded that the largest effect of DNQ photolysis on dissolution is the rearrangement of DNQ to be base-soluble. The presence of base-soluble ICA increases the dissolution rate compared with the unexposed state.

SUMMARY AND CONCLUSION

A working formulation of a positive-tone, aqueous-developable PNB resist has been presented. This formulation can be imaged in thick film form with good lithographic properties. The highest contrast achieved was 2.3, and the sensitivity (D_{100}) of was 408 mJ cm^{-2}. The maximum obtainable aspect ratio was calculated to be 3 : 2. Several factors affect the film quality and lithographic properties including the monomer ratio, PAC type, and PAC loading. It was observed that the PAC ballast molecule greatly affects its miscibility with the PNB films. NBCBA had better miscibility with PACs than NBFA. A problematic brown film was reported and evidence was given to support the hypothesis of a DNQ/ICA reaction. The effect of monomer ratio on the dissolution of PNB films was studied. It was shown that PAC causes a decrease in the dissolution rate of the exposed and unexposed PNBFA and 90/10% P(NBFA-NBCBA) films. It was also shown that increasing the NBCBA content of the film increased the dissolution rate of the film but also caused swelling of the unexposed regions. These dissolution characteristics are unique to these PNB polymers. FTIR analysis of the films showed that the addition of DNQ does not change the degree of hydrogen bonding appreciably. Further, exposure of the DNQ-containing films does not change the degree of hydrogen bonding.

REFERENCES

1. Maier, G. *Prog. Polym. Sci.* **2001,** *26*, 3.
2. Willson, C. G. *Microelectron. Eng.* **1983,** *1*, 269.
3. Wanat, S. F. *J Micro/Nanolithograph MEMS MOEMS* **2008,** *7*, 033008/033001.
4. Rajarathinam, V. *J Electron. Mater.* **2009,** *38*, 778.
5. Hsu, L.-C. J. *Appl. Polym. Sci.* **2003,** *90*, 2293.
6. Jin, X. Z. *J. Appl. Polym. Sci.* **2005,** *98*, 15.
7. Bai, Y. J. *Appl. Polym. Sci.* **2004,** *91*, 7.
8. Raeis-Zadeh, M. J. *Appl. Polym. Sci.* **2010,** *120*, 1916.
9. Ludovice, P. J. *Macromol. Theory Simul.* **2010,** *19*, 421.
10. Amoroso, D. *(U. S. Patent and Trademark Office). U. S. Pat. 7,858,721 (***2010).**
11. Toriumi, M. *Proc. SPIE* **2002,** *4690*, 904.
12. Reiser, A. *Macromolecules* **1994,** *27*, 7.
13. Reiser, A. *Macromolecules* **1995,** *28*, 6.
14. Reiser, A. *Macromolecules* **1998,** *31*, 5.
15. Mack, C. *Appl. Opt.* **1988,** *27*, 4913.
16. Vleggaar, J. J. *M. J. Vac. Sci. Technol. B* **1993,** *11*, 11.
17. Tanigaki, K. *Polym. Mater. Sci. Eng.* **1989,** *61*, 291.
18. Hinsberg, W. D. *Proc. SPIE* **2001,** *4345*, 1.
19. Hinsberg, W. D. *Macromolecules* **2005,** *38*, 1882.
20. Reiser, A. *Macromolecules* **1999,** *32*, 6.
21. Henderson, C. L. *Macromolecules* **2004,** *37*, 4512.
22. Ito, H. *Proc. SPIE* **2003,** *5039*, 70.
23. Reiser, A. *Macromolecules* **1998,** *31*, 8789.